

Analog Versus Hybrid Precoding for Multiuser Massive MIMO with Quantized CSI Feedback

Yaqiong Zhao, *Student Member, IEEE*, Wei Xu, *Senior Member, IEEE*, Jindan Xu, *Student Member, IEEE*, Shi Jin, *Senior Member, IEEE*, Kezhi Wang, *Member, IEEE*, and Mohamed-Slim Alouini, *Fellow, IEEE*

Abstract

In this letter, we study the performance of a downlink multiuser massive multiple-input multiple-output (MIMO) system with sub-connected structure over limited feedback channels. Tight rate approximations are theoretically analyzed for the system with pure analog precoding and hybrid precoding. The effect of quantized analog and digital precoding is characterized in the derived expressions. Furthermore, it is revealed that the pure analog precoding outperforms the hybrid precoding using maximal-ratio transmission (MRT) or zero forcing (ZF) under certain conditions, and we theoretically characterize the conditions in closed form with respect to signal-to-noise ratio (SNR), the number of users and the number of feedback bits. Numerical results verify the derived conclusions on both Rayleigh channels and mmWave channels.

Index Terms

Massive MIMO, analog precoding, hybrid precoding, limited feedback.

I. INTRODUCTION

MASSIVE multiple-input multiple-output (MIMO) has attracted increasing attention as a key technology in the fifth-generation (5G) network [1]. With its advantages for inter-user interference

Y. Zhao, J. Xu, and S. Jin are with the National Mobile Communications Research Laboratory, Southeast University, Nanjing 210096, China (email: {zhaoyaqiong, jdxu, jinshi}@seu.edu.cn).

W. Xu is with the National Mobile Communications Research Laboratory, Southeast University, Nanjing 210096, China, and is also with the Purple Mountain Laboratories, Nanjing 210000, China (wxu@seu.edu.cn).

K. Wang is with the Department of Computer and Information Sciences, Northumbria University, Newcastle, UK (email: kezhi.wang@northumbria.ac.uk).

M. -S. Alouini are with the Computer, Electrical and Mathematical Science and Engineering Division, King Abdullah University of Science and Technology, Thuwal, Saudi Arabia, 23955 (email: slim.alouini@kaust.edu.sa).

cancellation and noise suppression, massive MIMO can achieve near-optimal performance with simple linear precoding schemes, such as maximal-ratio transmission (MRT) and zero forcing (ZF) [2]. These fully-digital precoding schemes need each antenna to be driven by one dedicated radio-frequency (RF) chain, which imposes prohibitively high cost and power consumption [3]. To address this issue, two kinds of designs have been introduced, i.e., pure analog precoding and hybrid analog-and-digital precoding [4] [5].

Although the hybrid precoding has been widely considered in research, evidence has shown that it may not be the best choice for all cases compared with the pure analog precoding, especially when considering that analog precoding consumes less power than the hybrid precoding due to some implementation facts [4] [6]. In [7] [8], the analog precoding approximately transformed the effective channel into a diagonal matrix, which implies that digital processing is no longer needed for further multiuser interference cancellation. Specifically in [9], the authors found that pure analog processing could surpass the hybrid processing with maximal-ratio combination (MRC) or ZF in an uplink channel under the assumption of perfect channel state information (CSI). For the downlink channel, however, this compromise is still unclear. Moreover in practice, only quantized CSI, instead of perfect one, is available through limited feedback [10]-[13].

Against the above background, this letter investigates the performance of a downlink massive MIMO system with low-cost sub-connected architecture and quantized CSI feedback. Tight rate approximations are derived for the ZF/MRT-based hybrid precodings and the analog precoding in the large base station (BS) antenna regime. With the derived results, we explicitly characterize the performance comparison between the hybrid precoding and the analog precoding. In particular, we show that for all SNRs analog precoding outperforms the ZF-based hybrid precoding when $B_2 \leq B_2^0$ where B_2 denotes the number of feedback bits in digital precoding and B_2^0 is a constant in closed-form with respect to system parameters. Similar observation has also been obtained for the comparison of MRT-based hybrid precoding and pure analog precoding. For other cases, the superiority of different precoding schemes would be complicated and it depends on specific values of SNR, which has also been derived in closed forms.

The remainder of this paper is organized as follows. System model is introduced in Section II. In Section III, we derive the achievable rates of the system using various precoding schemes. In Section IV, we present the conditions under which the pure analog precoding can beat the hybrid precoding. Simulation results and conclusions are given in Section V and Section VI, respectively.

II. SYSTEM MODEL

We consider a multiuser massive MIMO downlink channel with sub-connected architecture. Multiple users are simultaneously served by a BS which is equipped with M antennas and K RF chains. Each RF chain is connected to a subset of N antennas through dedicated phase shifters where $N = \frac{M}{K}$. Considering that the number of transmit streams should not exceed the number of RF chains, we assume that K single-antenna users are scheduled from the user pool. Assuming flat Rayleigh fading, the received signal at the k th user can be expressed by

$$y_k = \beta_k \mathbf{h}_k^H \mathbf{A} \mathbf{W} \mathbf{s} + n_k, \quad k = 1, 2, \dots, K, \quad (1)$$

where $\mathbf{h}_k^H \sim \mathcal{CN}(\mathbf{0}_M, \mathbf{I}_M)$ denotes the downlink channel from the BS to the k th user, and $\mathbf{s} \in \mathbb{C}^{K \times 1}$ is the data vector with $\mathbb{E}[\mathbf{s} \mathbf{s}^H] = \frac{P}{K} \mathbf{I}_K$ where P is the total transmit power at the BS, $n_k \sim \mathcal{CN}(0, \sigma^2)$ is the additive Gaussian noise, β_k denotes the path loss of the k th user, and $\mathbf{A} = [\mathbf{a}_1, \mathbf{a}_2, \dots, \mathbf{a}_K] \in \mathbb{C}^{M \times K}$ and $\mathbf{W} = [\mathbf{w}_1, \mathbf{w}_2, \dots, \mathbf{w}_K] \in \mathbb{C}^{K \times K}$ respectively stand for the analog precoder and the digital precoder. Due to the hardware dissipation caused by the power dividers [14], the analog precoder is written as $\mathbf{A} = \frac{1}{\sqrt{N}} \mathbf{F}$ where \mathbf{F} denotes the equivalent analog precoding implemented by the phase shifter network. To conduct equal power allocation for users, it holds that $\|\mathbf{F} \mathbf{w}_k\| = 1$ for $k = 1, 2, \dots, K$.

In the current design of hybrid precoding for massive MIMO, the design of analog precoder can be accomplished in two ways, that is, by either utilizing a quantized CSI feedback from users, e.g., precoding matrix indicator (PMI) feedback, or by using uplink channel estimates, e.g., the sounding reference signal (SRS), as specified in the 5G New Radio (NR) specifications [15]. Based on this, the BS designs the analog precoder in terms of discretized phase shifters. Then, an analogly beamformed pilot will be sent by the BS for further equivalent channel estimation to compensate for the performance degradation caused by quantization error of the analog precoder. Each user estimates its own effective channel and feeds back a quantized version of the precoded CSI which is used by the BS to design the digital precoder. In this paper, phases of the MK entries of \mathbf{A} are quantized up to B_1 bits, i.e., the codebook is designed as $\mathcal{A} = \left\{ e^{\frac{j2\pi n}{2^{B_1}}}, n = 0, 1, \dots, 2^{B_1} - 1 \right\}$. Based on the minimum Euclidean distance criterion, a common way of analog precoder design in the sub-connected structure follows [9] [10]

$$a_{k,i} = \begin{cases} \frac{1}{N} \operatorname{argmax}_{e^{j\hat{\varphi}_{k,i}} \in \mathcal{A}} \mathcal{R}[h_{k,i}^* e^{j\hat{\varphi}_{k,i}}], & N(k-1) + 1 \leq i \leq Nk \\ 0, & \text{otherwise} \end{cases} \quad (2)$$

where $a_{k,i}$ and $h_{k,i}$ are respectively the i th element of \mathbf{a}_k and \mathbf{h}_k , and $\mathcal{R}[x]$ returns the real part of x . For the k th user, we define its effective channel as $\mathbf{g}_k^H \triangleq \mathbf{h}_k^H \mathbf{A}$. Then, the ergodic rate of the k th user can be written as

$$R_k = \mathbb{E} \left[\log_2 \left(1 + \frac{\frac{\gamma\beta_k}{K} |\mathbf{g}_k^H \mathbf{w}_k|^2}{1 + \frac{\gamma}{K} \sum_{j \neq k} \beta_j |\mathbf{g}_k^H \mathbf{w}_j|^2} \right) \right], \quad (3)$$

where $\gamma \triangleq \frac{P}{\sigma^2}$ is the SNR.

The digital part of the system is based on the effective channel. Since the effective channel is always correlated even for independent and identically distributed (i.i.d.) channels of \mathbf{H} , we adopt a channel statistics-based codebook \mathcal{G} [10]-[12]. The k th user quantizes its effective channel \mathbf{g}_k according to $\hat{\mathbf{g}}_k = \arg \max_{\hat{\mathbf{g}}_k^i \in \mathcal{G}} |\mathbf{g}_k^H \hat{\mathbf{g}}_k^i|$, in which $\hat{\mathbf{g}}_k^i$ is defined as

$$\hat{\mathbf{g}}_k^i = \frac{\mathbf{R}_k^{\frac{1}{2}} \mathbf{v}_i}{\|\mathbf{R}_k^{\frac{1}{2}} \mathbf{v}_i\|}, \quad (4)$$

where \mathbf{R}_k denotes the correlation matrix of user k 's effective channel and $\mathbf{v}_i \in \mathbb{C}^{K \times 1}$, $i \in \{1, 2, \dots, 2^{B_2}\}$ is an i.i.d. complex Gaussian vector randomly chosen from random vector quantization (RVQ) codebook of size 2^{B_2} . With the limited feedback of B_2 bits, the BS calculates the digital precoder by using the quantized CSI feedback $\hat{\mathbf{g}}_k$.

III. ACHIEVABLE RATE ANALYSIS

A. MRT/ZF-based Hybrid Precoding with Limited Feedback

For the MRT-based hybrid precoding, the digital precoder of user k is determined as

$$\mathbf{w}_k = \hat{\mathbf{g}}_k. \quad (5)$$

With the design above, we derive the downlink rate in the following theorem.

Theorem 1: Tight rate approximation of MRT-based hybrid precoding in the large BS antenna regime is obtained as

$$R_{H,k}^{\text{MRT}} = \log_2 \left(1 + \frac{\frac{\gamma\beta_k}{K} \left(\frac{\pi \text{sinc}^2(\delta)}{4} + \frac{K}{N} - \frac{2^{-\frac{B_2}{K-1}}}{N} \right) \left(\frac{\pi N \text{sinc}^2(\delta)}{4} + K \right)}{\frac{\pi N \text{sinc}^2(\delta)}{4} + K + \frac{\gamma}{K} \bar{\beta}_k \left(\frac{K}{N} + \frac{\pi \text{sinc}^2(\delta)}{2} \right)} \right), \quad (6)$$

where $\delta \triangleq \frac{\pi}{2^{B_1}}$, $\text{sinc}(x) \triangleq \frac{\sin(x)}{x}$ and $\bar{\beta}_k = \sum_{j \neq k} \beta_j$.

Proof. See Appendix A. □

From the above theorem, we can also get the achievable rate of the MRT-based hybrid system with perfect CSI as a special case by letting $B_1 \rightarrow \infty$ and $B_2 \rightarrow \infty$ in (6). It yields

$$R_{H,k}^{\text{MRT}_p} = \log_2 \left(1 + \frac{\frac{\gamma\beta_k N}{K} \left(\frac{\pi}{4} + \frac{K}{N}\right)^2}{\frac{\pi N}{4} + K + \frac{\gamma\bar{\beta}_k}{K} \left(\frac{\pi}{2} + \frac{K}{N}\right)} \right). \quad (7)$$

Note that this result coincides with the result in [9, Eq. (15)] except for that the signal term and the interference term calculated in [9] have an additional factor of $\frac{1}{N}$ if we let $\beta_i = 1, i = 1, 2, \dots, K$, which is because we consider the effect of the divider network.

For the ZF-based precoding, the digital precoder equals

$$\mathbf{W}^{\text{ZF}} = \hat{\mathbf{G}}(\hat{\mathbf{G}}^H \hat{\mathbf{G}})^{-1}, \quad (8)$$

where $\hat{\mathbf{G}} = [\hat{\mathbf{g}}_1, \hat{\mathbf{g}}_2, \dots, \hat{\mathbf{g}}_K]$ and $\mathbf{W}^{\text{ZF}} = [\mathbf{w}_1^{\text{ZF}}, \mathbf{w}_2^{\text{ZF}}, \dots, \mathbf{w}_K^{\text{ZF}}]$. The digital precoder is then normalized as $\mathbf{w}_k = \frac{\mathbf{w}_k^{\text{ZF}}}{\|\mathbf{F}\mathbf{w}_k^{\text{ZF}}\|}$. A tractable and tight bound of its achievable rate is given in the following proposition.

Proposition 1: The ergodic rate of the ZF-based hybrid precoding is asymptotically lower bounded by

$$R_{H,k}^{\text{ZF}} \geq \log_2 \left(\frac{4KN + \pi N \gamma \beta_k \text{sinc}^2(\delta)}{4KN + 4\gamma\bar{\beta}_k 2^{-\frac{B_2}{K-1}}} \right). \quad (9)$$

Proof. See Appendix B. □

B. Pure Analog Precoding

When the pure analog precoding is applied, the digital precoding matrix reduces to an identity matrix, i.e., $\mathbf{W} = \mathbf{I}_K$. Then we can easily get the following proposition.

Proposition 2: Tight rate approximation of the pure analog precoding in the large BS antenna regime is characterized as

$$R_{A,k} = \log_2 \left(1 + \frac{\gamma\beta_k \left(\frac{\pi N \text{sinc}^2(\delta)}{4} + 1\right)}{KN + \gamma\bar{\beta}_k} \right). \quad (10)$$

Proof. With the pure analog precoding, $\mathbb{E}[|\mathbf{g}_k^H \mathbf{w}_k|^2] = \mathbb{E}[|g_{k,k}|^2] = \frac{\pi \text{sinc}^2(\delta)}{4} + \frac{1}{N} - \frac{\pi \text{sinc}^2(\delta)}{4N}$ and $\mathbb{E}[|\mathbf{g}_k^H \mathbf{w}_j|^2] = \mathbb{E}[|g_{k,i}|^2] = \frac{1}{N}$. By applying [16, Lemma 1], and substituting these two expressions into (3) and using similar manipulations as that in the last step of (30), the proof completes. □

As a special case, we have the achievable rate of the system with perfect CSI by letting $B_1 \rightarrow \infty$, which gives

$$R_{A,k}^{\text{P}} = \log_2 \left(1 + \frac{\frac{\pi N \gamma \beta_k}{4}}{KN + \gamma\bar{\beta}_k} \right), \quad (11)$$

which consists with the existing result in [9, Eq. (13)].

IV. PURE ANALOG VS HYBRID PRECODING

To compare the performance of the pure analog precoding and the hybrid precoding, we evaluate the rate gap as

$$\Delta R = R_{\text{H},k}^X - R_{\text{A},k}, \quad (12)$$

where $X \in \{\text{ZF}, \text{MRT}\}$ represents the strategy of the digital precoding in the hybrid precoding.

A. MRT-based Hybrid Precoding

By letting $\Delta R \geq 0$, and substituting (6) and (10) into (12), we get

$$\frac{\gamma \bar{\beta}_k}{K} \left(\frac{K - 2 - 2^{-\frac{B_2}{K-1}}}{N} - \frac{\pi \text{sinc}^2(\delta)}{4} \right) > 2^{-\frac{B_2}{K-1}} - K + 1. \quad (13)$$

It implies that the MRT-based hybrid precoding outperforms the pure analog precoding if (13) holds. It is obvious that the right hand side of (13) is negative when $K > 1$. Checking that $\frac{K - 2 - 2^{-\frac{B_2}{K-1}}}{N} \geq \frac{\pi \text{sinc}^2(\delta)}{4}$, we can rewrite (13) as

$$K \geq \frac{\pi N \text{sinc}^2(\delta)}{4} + 2^{-\frac{B_2}{K-1}} + 2, \quad (14)$$

under which the MRT-based hybrid precoding outperforms the pure analog precoding for all SNR values. This is due to the fact that multiuser interference becomes a dominant factor when K becomes large, and the hybrid precoding which utilizes digital processing to eliminate interference enjoys a better performance than the pure analog precoding.

Moreover from (14), it is revealed that B_2 has a marginal impact on the performance of the MRT-based hybrid precoding since $2^{-\frac{B_2}{K-1}} \ll 1$. Therefore we can focus on the impact of B_1 on system performance. By applying Taylor's expansion to $\text{sinc}^2(\delta)$ with $\delta = \frac{\pi}{2^{B_1}}$, we get $\text{sinc}^2(\frac{\pi}{2^{B_1}}) \approx 1 - \frac{(\frac{\pi}{2^{B_1}})^2}{3}$, and (14) is further equivalent to

$$B_1 \leq \frac{1}{2} \log_2 \left(\frac{\pi^3 N}{3\pi N - 12 \left(K - 2 - 2^{-\frac{B_2}{K-1}} \right)} \right) \triangleq B_1^0. \quad (15)$$

Otherwise, when $B_1 > B_1^0$, it is not difficult to get

$$\Delta R \begin{cases} > 0, & \gamma < \gamma_0 \\ \leq 0, & \gamma \geq \gamma_0 \end{cases} \quad (16)$$

where $\gamma_0 \triangleq \frac{M \left(2^{-\frac{B_2}{K-1}} - K + 1 \right)}{\bar{\beta}_k \left(K - 2 - 2^{-\frac{B_2}{K-1}} - \frac{\pi N \text{sinc}^2(\delta)}{4} \right)}$.

Remark 1: When $B_1 \leq B_1^0$, the MRT-based hybrid precoding always outperforms the pure analog precoding in terms of the ergodic achievable rate for all SNRs. Otherwise the MRT-based hybrid precoding can beat the pure analog precoding only for low SNRs satisfying $\gamma < \gamma_0$.

B. ZF-based Hybrid Precoding

Similarly by letting $\Delta R \geq 0$ for $X = \text{ZF}$ in (12) and using (9) and (10), we obtain

$$B_2 > (K-1) \log_2 \left(1 + \frac{4(\beta_k + \bar{\beta}_k)}{\pi N \beta_k \text{sinc}^2(\delta)} \right) \triangleq B_2^0, \quad (17)$$

which uses the fact that $\frac{\pi N \beta_k \text{sinc}^2(\delta) \left(1 - 2^{-\frac{B_2}{K-1}} \right)}{4} > 2^{-\frac{B_2}{K-1}} (\beta_k + \bar{\beta}_k)$. When $B_2 > B_2^0$, it holds true that

$$\Delta R \begin{cases} > 0, & \gamma > \gamma_1 \\ \leq 0, & \gamma \leq \gamma_1 \end{cases} \quad (18)$$

where $\gamma_1 \triangleq \frac{4M(\bar{\beta}_k 2^{-\frac{B_2}{K-1}} + \beta_k)}{\bar{\beta}_k \left(\pi N \beta_k \text{sinc}^2(\delta) \left(1 - 2^{-\frac{B_2}{K-1}} \right) - 4(\beta_k + \bar{\beta}_k) 2^{-\frac{B_2}{K-1}} \right)}$.

Otherwise, when $B_2 \leq B_2^0$, the pure analog precoding always outperforms the ZF-based hybrid precoding for all SNRs. This is because the precoding vector of the k th user is supposed to lie in the null space of channels of other users and thus the ZF-based hybrid precoding is more dependent on the accuracy of channel estimation to cancel out interference.

Remark 2: If $B_2 \leq B_2^0$, the pure analog precoding beats the ZF-based hybrid precoding for all SNRs. Otherwise the ZF-based hybrid precoding takes over for high SNRs satisfying $\gamma \geq \gamma_1$.

V. SIMULATION RESULTS

In this section, we compare the downlink performance of the analog precoding and hybrid precoding based on different linear processing schemes. The path loss factor β_k , $k = 1, 2, \dots, K$ is chosen uniformly in $[0.5, 1.5]$.

A. Rayleigh Fading Channels

In Fig. 1(a) we illustrate the spectral efficiency achieved by pure analog precoding and the MRT-based hybrid precoding. It is observed that when $B_1 \leq B_1^0 = 1.05$, the MRT-based hybrid precoding outperforms

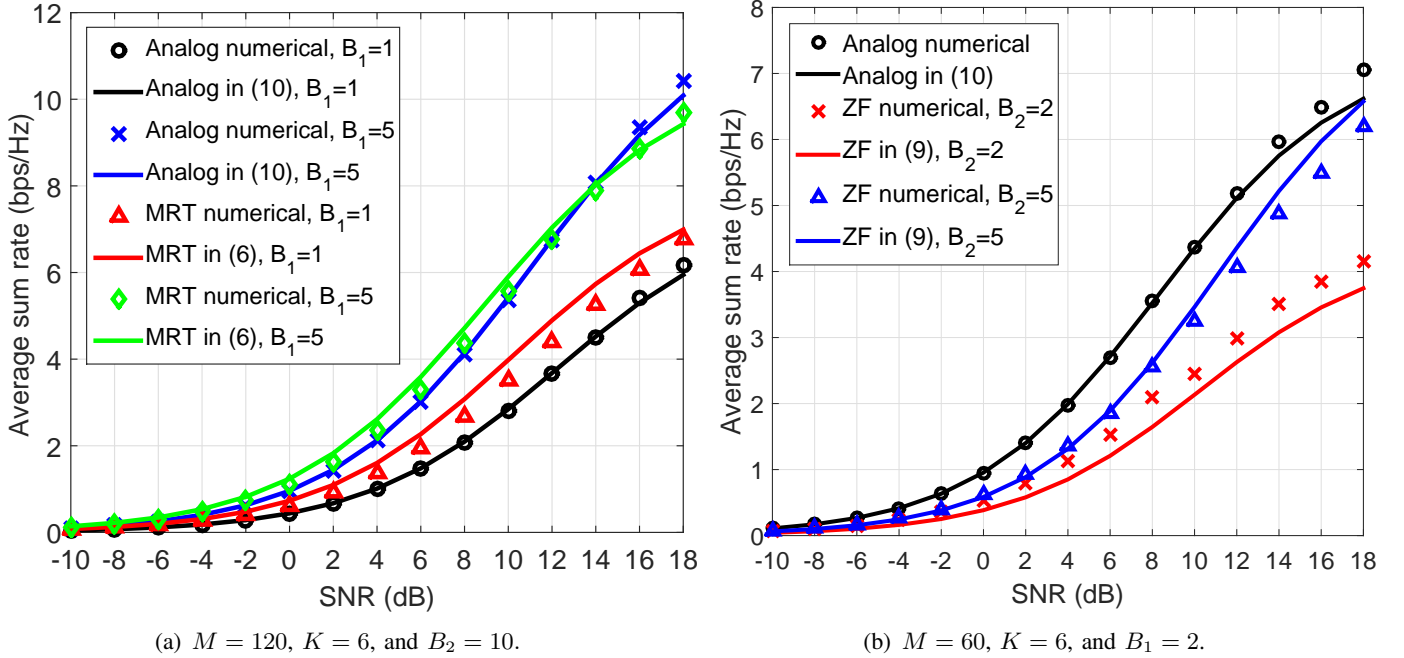


Fig. 1. Achievable rates of analog precoding and MRT-based hybrid precoding in (a) and ZF-based hybrid precoding in (b)

pure analog precoding for all SNRs, while when $B_1 > B_1^0$ the pure analog precoding performs better at high SNRs, confirming the conclusions in Section IV. This is because for small B_1 , the system performance is severely affected by the quantization error, i.e., the interference becomes dominant, thus the hybrid precoding using digital processing to eliminate interference outperforms the pure analog precoding. In addition, the corresponding threshold calculated from (14) is 17 for $B_1 = 5$, so for $K = 6 < 17$, the pure analog precoding outperforms the MRT-based hybrid precoding at high SNRs.

Similar trends can be found when comparing pure analog precoding and the ZF-based hybrid precoding in Fig. 1(b). When the effective channel is roughly quantized, i.e., $B_2 \leq B_2^0 = 4.29$, the pure analog precoding performs better for all SNRs since the accuracy of channel estimation is insufficient to support effective beamforming for ZF, while the ZF-based hybrid precoding takes over at high SNRs when $B_2 > B_2^0$, which verifies our observations in Section IV.

B. Large mmWave Multiuser Channels

Apart from Rayleigh fading channels, hybrid/analog precoding can also be applied to mmWave communications. To capture the nature of high-frequency propagations, we adopt the widely-used geometric channel model [7] [9]

$$\mathbf{h}_k^H = \sqrt{\frac{M}{N_p}} \sum_{l=1}^{N_p} \alpha_l^k \mathbf{a}^H(\phi_l^k), \quad (19)$$

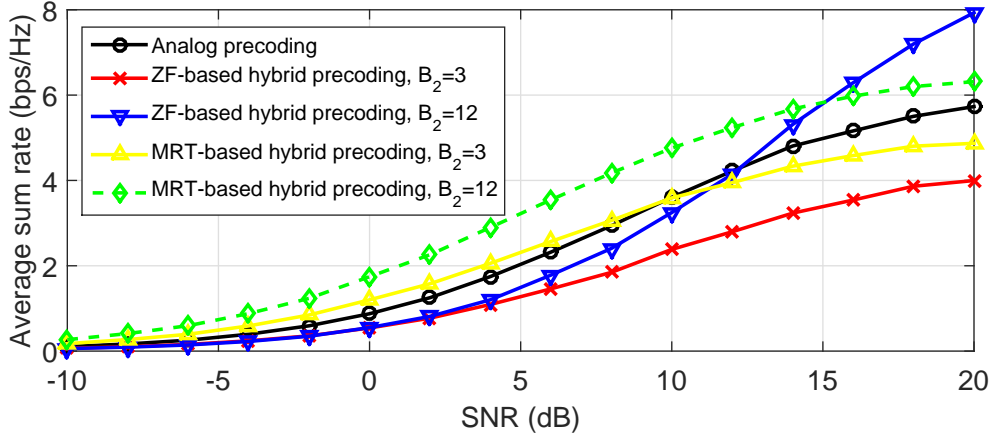


Fig. 2. Achievable rates over mmWave channels with $M = 40$, $K = 5$, $B_1 = 2$, and $N_p = 10$.

where N_p is the number of propagation paths from BS to user and $\alpha_l^k \sim \mathcal{CN}(0, 1)$ denotes the complex gain of the l -th path. ϕ_l^k is the azimuth angle of departure drawn independently from the uniform distribution over $[0, 2\pi]$. $\mathbf{a}(\phi_l^k)$ is the array response vector of BS. Here we consider a uniform linear array (ULA) whose array response vector is given by [9, eq. (29)].

Fig. 2 shows that conclusions on the superiority of the pure analog precoding over hybrid precodings also hold for the mm-Wave channels. Specifically, when B_2 is small, i.e., $B_2 = 3$, the analog precoding outperforms the ZF-based hybrid precoding for all SNRs, while for large B_2 , i.e., $B_2 = 12$, the ZF-based hybrid precoding takes over at high SNRs, which verifies Remark 2.

VI. CONCLUSION

In this paper, we derive tight rate approximations of a massive MIMO system using pure analog precoding and hybrid precoding with limited feedback in the large BS antenna regime. The effect of quantized analog and digital precodings are characterized in the obtained expressions. Furthermore, it is revealed that pure analog precoding outperforms hybrid precoding in terms of the ergodic achievable rate under certain conditions, which have been derived in closed forms with respect to the SNR, the number of users and the number of feedback bits. Numerical results verify the observed.

APPENDIX A

PROOF OF THEOREM 1

To evaluate (3), we calculate the terms $\mathbb{E} [|\mathbf{g}_k^H \mathbf{w}_k|^2]$ and $\mathbb{E} [|\mathbf{g}_k^H \mathbf{w}_j|^2]$. Let $\mathbf{g}_k = \|\mathbf{g}_k\| \tilde{\mathbf{g}}_k$ where $\tilde{\mathbf{g}}_k$ is the normalized \mathbf{g}_k , then we have $\mathbb{E} [|\mathbf{g}_k^H \mathbf{w}_k|^2] = \mathbb{E} [\|\mathbf{g}_k\|_F^2] \mathbb{E} [|\tilde{\mathbf{g}}_k^H \mathbf{w}_k|^2]$.

From the definition of \mathbf{g}_k , its k th element equals

$$g_{k,k} = \frac{1}{N} \sum_{l=N(k-1)+1}^{Nk} h_{k,l} e^{-j\hat{\varphi}_{k,l}} \stackrel{(a)}{=} \frac{1}{N} \sum_{l=N(k-1)+1}^{Nk} \lambda_l, \quad (20)$$

where (a) uses $\lambda_l \triangleq h_{k,l} e^{-j\hat{\varphi}_{k,l}}$. Defining $\varepsilon_{k,l} \triangleq \varphi_{k,l} - \hat{\varphi}_{k,l}$, it yields $\lambda_l = |h_{k,l}| e^{j\varepsilon_{k,l}}$. Recall $\mathbf{h}_k^H \sim \mathcal{CN}(\mathbf{0}_M, \mathbf{I}_M)$, where $\{h_{k,i}\}$'s are i.i.d. complex Gaussian variables with zero mean and unit variance. It implies that $|h_{k,l}|$ follows the Rayleigh distribution with mean $\frac{\sqrt{\pi}}{2}$ and variance $1 - \frac{\pi}{4}$. The quantization error $\varepsilon_{k,l} \sim U[-\delta, \delta]$ is a uniform distribution with $\delta \triangleq \frac{\pi}{2B_1}$. Then we have

$$\mathbb{E}[\mathcal{R}[\lambda_l]] = \mathbb{E}[\mathcal{R}[|h_{k,l}| e^{j\varepsilon_{k,l}}]] = \mathbb{E}[|h_{k,l}| \cos(\varepsilon_{k,l})] \stackrel{(a)}{=} \mathbb{E}[|h_{k,l}|] \mathbb{E}[\cos(\varepsilon_{k,l})] \stackrel{(b)}{=} \frac{\sqrt{\pi} \text{sinc}(\delta)}{2}, \quad (21)$$

where (a) utilizes the independence between $|h_{k,l}|$ and $\varepsilon_{k,l}$, and (b) is due to $\mathbb{E}[|h_{k,l}|] = \frac{\sqrt{\pi}}{2}$ and $\mathbb{E}[\cos(\varepsilon_{k,l})] = \frac{1}{2\delta} \int_{-\delta}^{\delta} \cos \varepsilon_{k,l} d\varepsilon_{k,l} = \text{sinc}(\delta)$ because of the given distributions of $|h_{k,l}|$ and $\varepsilon_{k,l}$. Analogously, we can also get $\mathbb{E}[(\mathcal{R}[\lambda_l])^2] = \mathbb{E}[|h_{k,l}|^2] \mathbb{E}[\cos^2(\varepsilon_{k,l})] = \frac{1+\text{sinc}(\delta)\cos(\delta)}{2}$. Then,

$$\mathbb{V}[\mathcal{R}[\lambda_l]] = \mathbb{E}[(\mathcal{R}[\lambda_l])^2] - (\mathbb{E}[\mathcal{R}[\lambda_l]])^2 = w_1, \quad (22)$$

where $w_1 \triangleq \frac{1+\text{sinc}(\delta)\cos(\delta)}{2} - \frac{\pi \text{sinc}^2(\delta)}{4}$. Applying the Central Limit Theorem to (20) and using (21) and (22), we get

$$\mathcal{R}[g_{k,k}] \sim \mathcal{N}\left(\frac{\sqrt{\pi} \text{sinc}(\delta)}{2}, \frac{w_1}{N}\right). \quad (23)$$

Following similar reasons, it can be readily proved that

$$\mathcal{I}[g_{k,k}] \sim \mathcal{N}\left(0, \frac{w_2}{N}\right), \quad \mathcal{R}[g_{k,i}] \sim \mathcal{N}\left(0, \frac{1}{2N}\right), \quad \mathcal{I}[g_{k,i}] \sim \mathcal{N}\left(0, \frac{1}{2N}\right), \quad (24)$$

where $w_2 \triangleq \frac{1-\text{sinc}(\delta)\cos(\delta)}{2}$ and $\mathcal{I}[x]$ returns the imaginary part of x . Now we have

$$\mathbb{E}[|g_{k,k}|^2] = \mathbb{E}[|\mathcal{R}[g_{k,k}]|^2] + \mathbb{E}[|\mathcal{I}[g_{k,k}]|^2] = \frac{\pi \text{sinc}^2(\delta)}{4} + \frac{w_1 + w_2}{N}. \quad (25)$$

$$\mathbb{E}[|g_{k,i}|^2] = \mathbb{E}[|\mathcal{R}[g_{k,i}]|^2] + \mathbb{E}[|\mathcal{I}[g_{k,i}]|^2] = \frac{1}{N}. \quad (26)$$

According (25) and (26), it gives

$$\mathbb{E}[\|\mathbf{g}_k\|_{\text{F}}^2] = \mathbb{E}[|g_{k,k}|^2] + \sum_{i=1, i \neq k}^K \mathbb{E}[|g_{k,i}|^2] = \frac{\pi \text{sinc}^2(\delta)}{4} + \frac{K}{N} - \frac{\pi \text{sinc}^2(\delta)}{4N}. \quad (27)$$

From [10, Lemma 2], \mathbf{R}_k can be asymptotically written as $\mathbf{R}_k = \text{diag}[r_{1,1}, r_{2,2}, \dots, r_{k,k}]$ where

$$r_{i,i} = \begin{cases} \frac{\pi \text{sinc}^2(\delta)}{4} + \frac{1}{N} - \frac{\pi \text{sinc}^2(\delta)}{4N}, & i = k \\ \frac{1}{N}, & i \neq k \end{cases} \quad (28)$$

and $\text{diag}[\cdot]$ returns a diagonal matrix with the input as its elements. Then we follow the result in [11] and get

$$\mathbb{E} \left[\left| \tilde{\mathbf{g}}_k^H \hat{\mathbf{g}}_k \right|^2 \right] \approx 1 - \frac{\sigma_{k,2}^2}{\sigma_{k,1}^2} 2^{-\frac{B_2}{K-1}} = 1 - \frac{2^{-\frac{B_2}{K-1}}}{\frac{\pi N \text{sinc}^2(\delta)}{4} + 1 - \frac{\pi \text{sinc}^2(\delta)}{4}}, \quad (29)$$

where $\sigma_{k,1}$ and $\sigma_{k,2}$ respectively stand for the largest and the second largest singular value of $\mathbf{R}_k^{\frac{1}{2}}$.

Combining (27) and (29), it yields

$$\mathbb{E} \left[\left| \mathbf{g}_k^H \mathbf{w}_k \right|^2 \right] \stackrel{(a)}{=} \mathbb{E} \left[\left\| \mathbf{g}_k \right\|_F^2 \right] \mathbb{E} \left[\left| \tilde{\mathbf{g}}_k^H \hat{\mathbf{g}}_k \right|^2 \right] \stackrel{(b)}{\rightarrow} \frac{\pi \text{sinc}^2(\delta)}{4} + \frac{K}{N} - \frac{2^{-\frac{B_2}{K-1}}}{N},$$

where (a) utilizes $\mathbf{w}_k = \mathbf{g}_k$ and in (b) we consider the fact that $\frac{\frac{\pi \text{sinc}^2(\delta)}{4} + \frac{K}{N}}{\frac{\pi \text{sinc}^2(\delta)}{4} + \frac{K}{N} - \frac{\pi \text{sinc}^2(\delta)}{4N}} \rightarrow 1$ and $\frac{\frac{\pi \text{sinc}^2(\delta)}{4} + \frac{K}{N} - \frac{\pi \text{sinc}^2(\delta)}{4N}}{\frac{\pi N \text{sinc}^2(\delta)}{4} + 1 - \frac{\pi \text{sinc}^2(\delta)}{4}} \rightarrow \frac{1}{N}$ hold in massive MIMO with large N and fixed K .

From (4), we get $\hat{g}_{j,j} = \frac{(\mathbf{R}_j^{\frac{1}{2}})_{j,j} v_{i,j}}{\|\mathbf{R}_j^{\frac{1}{2}} \mathbf{v}_i\|}$, where $\hat{g}_{j,j}$ and $v_{i,j}$ are respectively the j th element of $\hat{\mathbf{g}}_j$ and \mathbf{v}_i , and i denotes the index of the quantization vector of \mathbf{g}_j . Then we have

$$\mathbb{E}[\hat{g}_{j,j}] = \mathbb{E} \left[\frac{(\mathbf{R}_j^{\frac{1}{2}})_{j,j} v_{i,j}}{\|\mathbf{R}_j^{\frac{1}{2}} \mathbf{v}_i\|} \right] \stackrel{(a)}{=} \mathbb{E}[v_{i,j}] \mathbb{E} \left[\frac{(\mathbf{R}_j^{\frac{1}{2}})_{j,j}}{\|\mathbf{R}_j^{\frac{1}{2}} \mathbf{v}_i\|} \right] \stackrel{(b)}{=} 0, \quad (30)$$

where (a) uses the independence between $v_{i,j}$ and $\frac{(\mathbf{R}_j^{\frac{1}{2}})_{j,j}}{\|\mathbf{R}_j^{\frac{1}{2}} \mathbf{v}_i\|}$, and (b) results from $\mathbf{v}_i \sim \mathcal{CN}(\mathbf{0}_M, \mathbf{I}_M)$.

Analogously,

$$\mathbb{E} \left[\left| \hat{g}_{j,j} \right|^2 \right] = \mathbb{E} \left[\frac{(\mathbf{R}_j)_{j,j} |v_{i,j}|^2}{\|\mathbf{R}_j^{\frac{1}{2}} \mathbf{v}_i\|^2} \right] = \mathbb{E} \left[|v_{i,j}|^2 \right] \frac{(\mathbf{R}_j)_{j,j}}{\mathbb{E} \left[\|\mathbf{R}_j^{\frac{1}{2}} \mathbf{v}_i\|^2 \right]} \stackrel{(a)}{=} \frac{\frac{\pi \text{sinc}^2(\delta)}{4} + \frac{1}{N} - \frac{\pi \text{sinc}^2(\delta)}{4N}}{\frac{\pi \text{sinc}^2(\delta)}{4} + \frac{K}{N} - \frac{\pi \text{sinc}^2(\delta)}{4N}}, \quad (31)$$

where (a) uses $\mathbb{E} \left[\|\mathbf{R}_j^{\frac{1}{2}} \mathbf{v}_i\|^2 \right] = \sum_{l=1}^K (\mathbf{R}_j)_{l,l} \mathbb{E} \left[|v_{i,l}|^2 \right] = \sum_{l=1}^K (\mathbf{R}_j)_{l,l} = \frac{\pi \text{sinc}^2(\delta)}{4} + \frac{K}{N} - \frac{\pi \text{sinc}^2(\delta)}{4N}$ and $\mathbb{E} \left[|v_{i,l}|^2 \right] = 1$ according to the distribution of \mathbf{v}_i and (28). Following trivially the above steps, we get $\mathbb{E}[\hat{g}_{j,i}] = 0$, and $\mathbb{E} \left[\left| \hat{g}_{j,i} \right|^2 \right] = \frac{1}{\frac{\pi N \text{sinc}^2(\delta)}{4} + K - \frac{\pi \text{sinc}^2(\delta)}{4}}$. Providing that $\{v_{i,l}\}$'s are i.i.d. complex Gaussian variables with zero mean and unit variance, then $\hat{g}_{j,i}$ and $\hat{g}_{j,l}$ are independent for any $i \neq l$, which implies $\mathbb{E}[\hat{g}_{j,i} \hat{g}_{j,l}^*] =$

$\mathbb{E}[\hat{g}_{j,i}]\mathbb{E}[\hat{g}_{j,l}^*] = 0$ and $\mathbb{E}[|\hat{g}_{j,i}|^2|\hat{g}_{j,l}^*|^2] = \mathbb{E}[|\hat{g}_{j,i}|^2]\mathbb{E}[|\hat{g}_{j,l}^*|^2]$. Then $\mathbb{E}\left[|\mathbf{g}_k^H \mathbf{w}_j|^2\right]$ can be calculated as

$$\begin{aligned} \mathbb{E}\left[|\mathbf{g}_k^H \mathbf{w}_j|^2\right] &= \mathbb{E}\left[|\mathbf{g}_k^H \hat{\mathbf{g}}_j|^2\right] = \mathbb{E}\left[\left|\sum_{i=1}^K g_{k,i}^* \hat{g}_{j,i}\right|^2\right] \stackrel{(a)}{=} \sum_{1 \leq i \leq l \leq K} \mathbb{E}[g_{k,i}^* g_{k,l}] \mathbb{E}[\hat{g}_{j,i} \hat{g}_{j,l}^*] \\ &\stackrel{(b)}{=} \sum_{i=1}^K \mathbb{E}[|\hat{g}_{j,i}|^2] \mathbb{E}[|g_{k,i}|^2] \stackrel{(c)}{\rightarrow} \frac{\frac{\pi \text{sinc}^2(\delta)}{2} + \frac{K}{N}}{\frac{\pi N \text{sinc}^2(\delta)}{4} + K}, \end{aligned} \quad (32)$$

where (a) is due to the independence between \mathbf{g}_k and $\hat{\mathbf{g}}_j$, (b) holds because $\mathbb{E}[g_{k,i}^* g_{k,l}] \mathbb{E}[\hat{g}_{j,i} \hat{g}_{j,l}^*] = 0$ for any $i \neq l$, and (c) is obtained by using similar manipulations as that in the last step of (30). Finally, by applying [16, Lemma 1] and substituting (30) and (32) into (3), the theorem is proved.

APPENDIX B

PROOF OF PROPOSITION 1

From the distributions of $g_{k,k}$ and $g_{k,i}$ in (23) – (24), we get $g_{k,k} \xrightarrow{a.s.} \frac{\sqrt{\pi \text{sinc}(\delta)}}{2}$ and $g_{k,i} \xrightarrow{a.s.} 0$ since $\frac{w_1}{N} \rightarrow 0$, $\frac{w_2}{N} \rightarrow 0$, and $\frac{1}{2N} \rightarrow 0$ for the massive MIMO with large N , thus $\mathbf{G} \xrightarrow{a.s.} \frac{\pi \text{sinc}^2(\delta)}{4} \mathbf{I}_K$. Now the asymptotic rate of the ZF-based hybrid system with perfect CSI can be represented as

$$R_{\text{H},k}^{\text{ZFP}} \xrightarrow{a.s.} \log_2 \left(1 + \frac{\gamma \beta_k \pi \text{sinc}^2(\delta)}{4K} \right). \quad (33)$$

On the other hand, it is known from [12] that the rate loss caused by the imperfect CSI can be upper bounded by $\log_2 \left(1 + \frac{\gamma \bar{\beta}_k \mathbb{E}[|\mathbf{g}_k^H \mathbf{w}_j|^2]}{K} \right)$. Thanks to the orthogonality between $\hat{\mathbf{g}}_k$ and \mathbf{w}_j in the ZF precoding, we further have

$$\mathbb{E}\left[|\mathbf{g}_k^H \mathbf{w}_j|^2\right] \leq \mathbb{E}\left[\|\mathbf{g}_k\|_{\text{F}}^2\right] \mathbb{E}\left[1 - |\tilde{\mathbf{g}}_k^H \hat{\mathbf{g}}_k|^2\right] = \frac{2^{-\frac{B_2}{K-1}}}{N}. \quad (34)$$

Therefore, we have

$$R_{\text{loss}} \leq \log_2 \left(1 + \frac{\gamma \bar{\beta}_k 2^{-\frac{B_2}{K-1}}}{KN} \right). \quad (35)$$

Combining (33) and (35), the proposition is directly proved.

REFERENCES

- [1] M. Wang, F. Gao, S. Jin, and H. Lin, "An overview of enhanced massive MIMO with array signal processing techniques," *IEEE J. Sel. Topics Signal Process.*, vol. 13, no. 5, pp. 886-901, Sept. 2019.
- [2] M. Matthaiou, C. Zhong, and T. Ratnarajah, "Novel generic bounds on the sum rate of MIMO ZF receivers," *IEEE Trans. Signal Process.*, vol. 59, no. 9, pp. 4341-4353, Sept. 2011.

- [3] X. Yu, J. C. Shen, J. Zhang, and K. B. Letaief, "Alternating minimization algorithms for hybrid precoding in millimeter wave MIMO systems," *IEEE J. Sel. Topics Signal Process.*, vol. 10, no. 3, pp. 485–500, Apr. 2016.
- [4] A. Alkhateeb, J. Mo, N. Gonzalez-Prelcic, and R. W. Heath, "MIMO precoding and combining solutions for millimeter-wave systems," *IEEE Commun. Mag.*, vol. 52, no. 12, pp. 122–131, Dec. 2014.
- [5] R. Ghanaatian, V. Jamali, A. Burg, and R. Schober, "Feedback-aware precoding for millimeter-wave massive MIMO systems," in *Proc. IEEE 30th Annu. Int. Symp. Pers. Indoor, Mobile Radio Commun.*, Sept. 2019, pp. 1–7.
- [6] C. Fang, B. Makki, J. Li, and T. Svensson. (2020, Jan 13). *Hybrid precoding in cooperative millimeter wave networks* [Online]. Available: <https://arxiv.org/abs/2001.04390v1>.
- [7] L. Liang, W. Xu, and X. Dong, "Low-complexity hybrid precoding in massive multiuser MIMO systems," *IEEE Wireless Commun. Lett.*, vol. 3, no. 6, pp. 653–656, Dec. 2014.
- [8] M. Fozooni, M. Matthaiou, S. Jin, and G. C. Alexandropoulos, "Massive MIMO relaying with hybrid processing," in *Proc. IEEE ICC*, Kuala Lumpur, Malaysia, May 2016, pp. 1–6.
- [9] J. Du, W. Xu, B. Sheng, and C. Zhao, "Rethinking uplink hybrid processing: When is pure analog processing suggested?" *IEEE Trans. Veh. Technol.*, vol. 68, no. 5, pp. 5139–5144, May 2019.
- [10] J. Du, W. Xu, H. Shen, X. Dong, and C. Zhao, "Hybrid precoding architecture for massive multiuser MIMO with dissipation: Sub-connected or fully-connected structures?" *IEEE Trans. Wireless Commun.*, vol. 17, no. 8, pp. 5465–5479, Aug. 2018.
- [11] B. Clerckx, G. Kim, and S. Kim, "MU-MIMO with channel statistics-based codebooks in spatially correlated channels," in *Proc. IEEE GLOBECOM 2008*, New Orleans, LA, USA, Dec. 2008, pp. 1–5.
- [12] W. Shen, L. Dai, Y. Zhang, J. Li, and Z. Wang, "On the performance of channel-statistics-based codebook for massive MIMO channel feedback," *IEEE Trans. Veh. Technol.*, vol. 66, no. 8, pp. 7553–7557, Aug. 2017.
- [13] H. Wang, W. Wang, V. K. N. Lau, and Z. Zhang, "Hybrid limited feedback in 5G cellular systems with massive MIMO," *IEEE Syst. J.*, vol. 11, no. 1, pp. 50–61, Mar. 2017.
- [14] V. Venkateswaran, F. Pivit, and L. Guan, "Hybrid RF and digital beamformer for cellular networks: Algorithms, microwave architectures, and measurements," *IEEE Trans. Microw. Theory Techn.*, vol. 64, no. 7, pp. 2226–2243, Jul. 2016.
- [15] A. Zaidi, G. Durisi, F. Athley, J. Medbo, X. Chen, and U. Gustavsson, *5G Physical Layer: Principles, Models and Technology Components*, Academic Press, 2018.
- [16] Q. Zhang, S. Jin, K. Wong, H. Zhu, and M. Matthaiou, "Power scaling of uplink massive MIMO systems with arbitrary-rank channel means," *IEEE J. Sel. Topics Signal Process.*, vol. 8, no. 5, pp. 966–981, Oct. 2014.